

Relationship between the CaF_2 (C 1) and CdCl_2 (C 19) Structure Types, with Assorted Remarks on C 19, Anti-C 19, and Related Compounds

OSVALD KNOP

Department of Chemistry, Dalhousie University, Halifax, Nova Scotia B3H 4J3, Canada

Received April 9, 1982

It is shown how the 6:(3 + 3)-coordinated AB_2 layer structure of the C 19 type can be derived by continuous rhombohedral distortion from the cubic 8:8-coordinated C 1-type structure. The magnitude of the distortion actually observed (as manifested in the c/a ratio per AB_2 layer, R_1) is considered in relation to geometric factors, with particular attention to the competing CdI_2 (C 6) structure type. Reasons are suggested for the nonoccurrence of the C 19 structure type among $M(\text{OH})_2$ and of the anti-C 19 type among the simple hexahalometallates(IV), A_2MX_6 . Finally, the structures of alkylammonium hexahalometallates(IV), $(R_n\text{NH}_{4-n})_2MX_6$, are surveyed to demonstrate how the charge arrangements of the composite cations and anions in these compounds are able to mimic the structure types encountered with simple AB_2 compounds.

Although the CdCl_2 -type (C 19) structure can be derived from the fluorite-type (C 1) structure in a straightforward manner by rhombohedral distortion,¹ oddly enough this is not pointed out in standard treatises on crystal or structural chemistry (3–8). On occasion (e.g., Ref. (9)) the term “rhombohedrally distorted fluorite structure” is encountered, which, while correct, does not reveal the C 19 structure as a natural alternative to the C 1 structure; references to cubic stacking sequences of layers in the C 1 and C 19 structures (e.g., Refs. (7, 10, 11)) suggest the relationship only obliquely. The connection between the two is perhaps obscured by the ingrained habit of regarding the C 1 structure as 8:4 coordinated and thus unrelated to the 6:(3 + 3) (or 6:3)-coordinated, layer-type C 19

structure. Our recent incursions into the systematic structural chemistry of bis(alkylammonium) hexachlorostannates(IV), $(R_n\text{NH}_{4-n})_2\text{SnCl}_6$ (Ref. (12) and results to be published), have convinced us of the desirability to demonstrate the relationship explicitly. This is done in the following, where we also compare structural features of compounds of these two and related types.

The C 19 Structure as a Distorted C 1 Structure

To display this relationship, the structure of an AB_2 fluorite ($Fm\bar{3}m$, $Z = 4$, unit-cell dimension a_F , A in $4(a)000$ etc., B in $8(c)000$ etc.) may be described in terms of a primitive rhombohedral cell of symmetry $R\bar{3}m$ ($Z = 1$, $a_{rh} = a_F/\sqrt{2}$, $\alpha = 60^\circ$, A in $1(a)000$, B in $2(c)000$ etc.) or the corresponding hexagonal cell (Z

¹ This was noted already by Goldschmidt (1, 2).

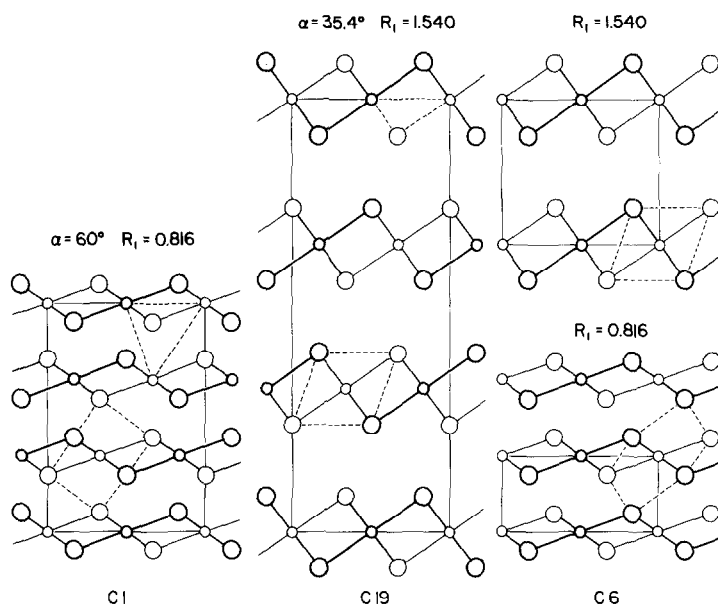


FIG. 1. AB_2 structures of the C 1 (CaF_2), C 19 (CdCl_2), and C 6 (CdI_2) types projected on $(11\bar{2}0)$. Small circles, A; large circles, B; thin outline, atoms in $(11\bar{2}0)$; heavy outline, two atoms out of $(11\bar{2}0)$, eclipsed; α , rhombohedral angle; $R_1 = c/a$ per AB_2 layer. Broken lines represent contours of the coordination polyhedra of A and B.

$= 3$, $a = a_{\text{rh}}$, $c = a_{\text{F}}\sqrt{3}$, A in $3(a) - 000$ etc. B in $6(c) - \pm(00z)$ etc., $z = X = \frac{1}{4}$). The fluorite structure in this presentation (Fig. 1) may be regarded as consisting of AB_2 layers in an $ABCABC \dots$ stacking sequence, with $c/a = R = \sqrt{6} \sim 2.449$, i.e., 0.816 per layer ($= R_1$). The C 19 structure results by relaxing the constraint on α and X , i.e., allowing α and X to assume values different from 60° and $\frac{1}{4}$, respectively. For $\alpha < 60^\circ$ (i.e., $R > \sqrt{6}$) and $X \sim \frac{1}{4}$, the separation between the layers increases. Simultaneously, the 8-coordination of A changes to 6-coordination, and the 4-coordination of B to 3-coordination (or $3 + 3$). For $\alpha > 60^\circ$ (i.e., $R < \sqrt{6}$ and $X \sim \frac{1}{4}$, the coordination numbers (c.n.) remain the same as in C 1, but the coordination of A now resembles the $(6+2)$ -coordination of the lower-charge cation in cubic pyrochlores. The changes produced by an increase in R are illustrated in Fig. 1.

The shortest interatomic distances in the C 19 structure are

$d(AB) = aRz$ (A, B on the same C_3 axis);

$d'(AB) = a[\frac{1}{3} + (\frac{1}{3} - z)^2 R^2]^{1/2}$ (A, B on neighboring C_3 axes);

$d(BB) = a$ (B, B in the same B layer);

$d'(BB) = a[\frac{1}{3} + 4(\frac{1}{3} - z)^2 R^2]^{1/2}$ (B, B on opposite sides of an AB_2 layer); and

$d''(BB) = a[\frac{1}{3} + (2z - \frac{1}{3})^2 R^2]^{1/2}$ (shortest B-B distances between AB_2 layers),

where $z = \frac{1}{4} + \delta$. In order that $d(AB) = d'(AB)$, $R = \frac{1}{3}(6z - 1)^{-1/2} = [\frac{1}{8}(1 + 12\delta)]^{-1/2}$; for a fluorite, $\delta = 0$, $R = \sqrt{6}$. For AB_6 to be a metrically regular octahedron, $d(BB) = d'(BB)$ and $R = (2/\sqrt{6})/(1 - 3z) = (2\sqrt{6})/(1 - 12\delta)$ or $\sin^2 \frac{1}{2}\alpha = 3\Delta^2/(4\Delta^2 + 3z)$, where $\Delta = 1 - 12\delta$. For $\delta = 0$ this yields $R = 2\sqrt{6}$, $R_1 \sim 1.633$, $\alpha \sim 33.56^\circ$.

Thus the passage from the 8:4 C 1 structure to the 6:3 C 19 layer structure is accomplished by a continuous, topology-preserving rhombohedral distortion of the cubic structure. The C 19 structure then emerges as a natural displacive alternative to the fluorite structure, and this is in keep-

ing with the well-known observation that the character of simple (i.e., with A , B not composite) AB_2 C 19 compounds is more ionic than that of the corresponding compounds having the other commonly occurring type of layer structure, CdI_2 (C 6).² One would expect the continuous nature of the geometric deformation process to be re-

² In the C 6 structure (Fig. 1) $d'(AB) = a[\frac{1}{3} + z^2R^2]^{1/2}$, $d''(AB) = a[\frac{1}{3} + (1 - z)^2R^2]^{1/2}$ (shortest distance between A and B in adjacent AB_2 layers), $d(BB) = a$, $d'(BB) = a[\frac{1}{3} + 4z^2R^2]^{1/2}$, $d''(BB) = a[\frac{1}{3} + (1 - 2z)^2R^2]^{1/2}$. While in the C 19 structure with $z \sim \frac{1}{4}$ 8-coordination of A is achieved by reducing R to $\sqrt{6}$, without the necessity of changing the value of z , in C 6 an increase in the c.n. of A can only be achieved by increasing z (Fig. 1). When $d'(AB) = d''(AB)$, $z = \frac{1}{2}$ and the coordination figure of A is a hexagonal prism AB_{12} and that of B a trigonal prism BA_6 , i.e., the C 6 structure goes over into the AlB_{12} (C 32)-type structure.

flected in a continuous (though not necessarily monotonic) variation of the Madelung constant, and hence the electrostatic energy, with R_1 and z .

Magnitude of the Distortion Actually Observed

The distribution of the observed R_1 values according to the mean linear unit-cell dimension $\bar{a} = (V/Z)^{1/3}$ is shown in Fig. 2.³ This plot is self-consistent in that it depends only on quantities derived directly from the crystallography of the compounds in question and not on external parameters. As might be expected, for simple AB_2 compounds the R_1 (C 19) values cluster about

³ Where no reference is given, details of the structural information will be found in Refs. (6, 7, or 13).

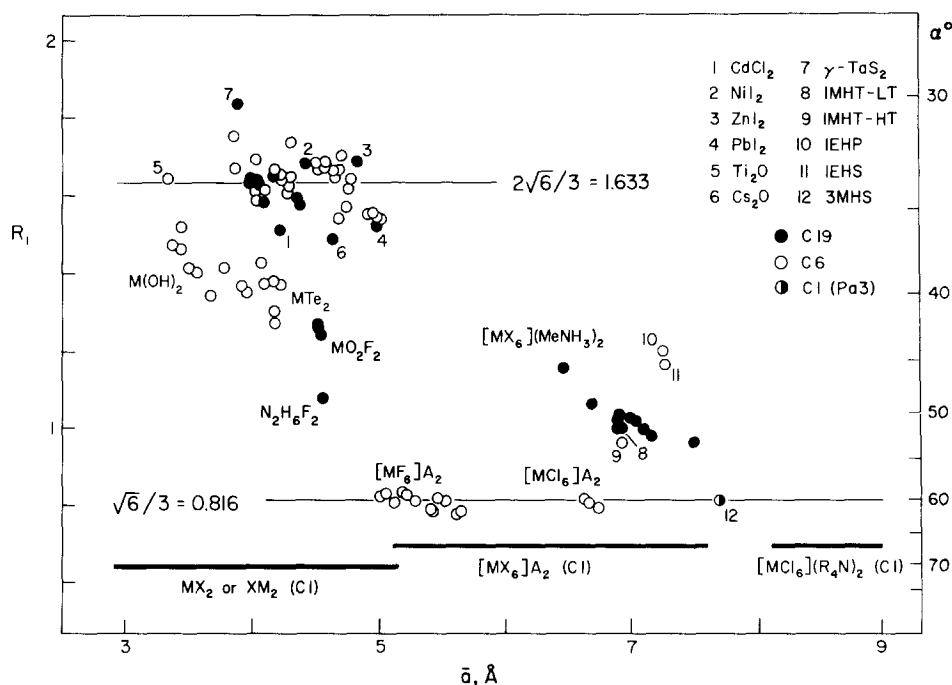


FIG. 2. Distribution of the C 1, C 19, and C 6 structures among $A^{2+}B_2^-$ and $A^{2-}B_2^-$ (anti) compounds according to the mean linear unit-cell dimension $\bar{a} = (V/Z)^{1/3}$ and R_1 (or the rhombohedral angle α). IMHT, $(MeNH_3)_2TeCl_6$, low- (LT) and high- (HT) temperature phases; IEHP, $(EtNH_3)_2PtCl_6$. The heavy horizontal bars (displaced from $R_1 = 0.816$ for clarity) indicate the \bar{a} existence ranges of compounds reported to have structures of the C 1 ($Fm\bar{3}m$) type.

$R_1 = \frac{2}{3}\sqrt{6} \sim 1.633$, the value corresponding to a metrically regular AB_6 octahedron. Notably different $R_1(C 19)$ values obtain for the anti-C 19 Cs_2O and for γ - TaS_2 , $CdCl_2$, and PbI_2 , although none of these compounds has an R_1 as low as the C 6-type $M(OH)_2$ and some of the MTe_2 . On the other hand, for the rhombohedrally distorted ordered fluorites $LnOF$ the R_1 values range from 0.826 (for Y) to only 0.831 (for La), i.e., from $\alpha = 59.5$ to 59.2° , if the structure is referred to the rhombohedral unit cell specified above. Thus, while the distortion of the fluorite structure into the $CdCl_2$ -type structure, geometrically, is a continuous process, for the simple C 1 and C 19 AB_2 structures actually observed there

is a gap in the R_1 variation, indicating that, *physically*, the two structure types correspond to two nonoverlapping stability ranges.

Clearly, at some point an abrupt change-over occurs from the C 1 to the C 19 structure type, such as from Rb_2O to Cs_2O . The existence of this discontinuous changeover is associated with both the relative and the absolute size of the participating atoms (Fig. 3). However, the point for Cs_2O in the r_A/r_B vs \bar{a} plot for simple AB_2 compounds⁴ almost falls on the continuation of the curve for the anti-C 1 M_2O ($M = Li, Na, K, Rb$), so the factors responsible for the sudden

⁴ Using Shannon's (14) $r^{vi}(Cs^+)$ derived from a set including CsF and compounds other than Cs_2O .

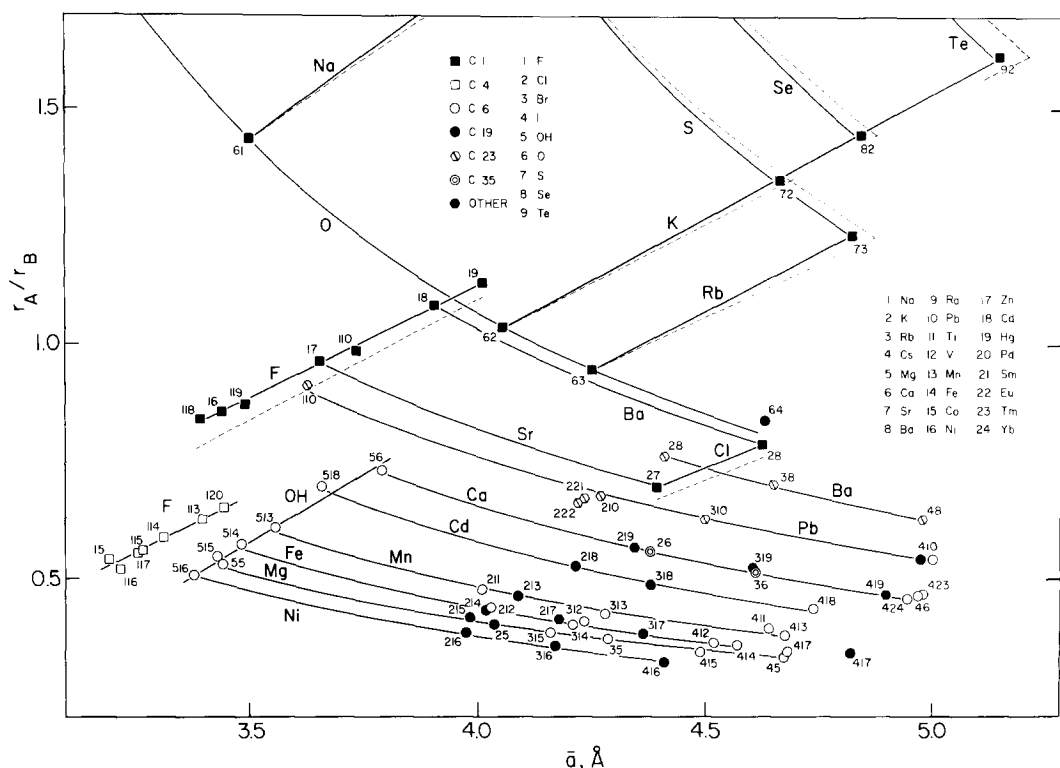


FIG. 3. Separation of the structure types for simple AB_2 halides, hydroxides, and M_2O alkali oxides according to the ionic-radius ratio r_A/r_B and the mean linear unit-cell dimension \bar{a} . The first digit of the code number refers to the anion, the following digit(s) to the cation. Solid straight lines, best linear fits for a particular B ; solid curves, best fits to $r_A/r_B = (k_1 \bar{a} - k_0)^{-1}$ for a particular A ; broken lines, $r_A/r_B = (K/r_B) \bar{a} - 1$ (see text).

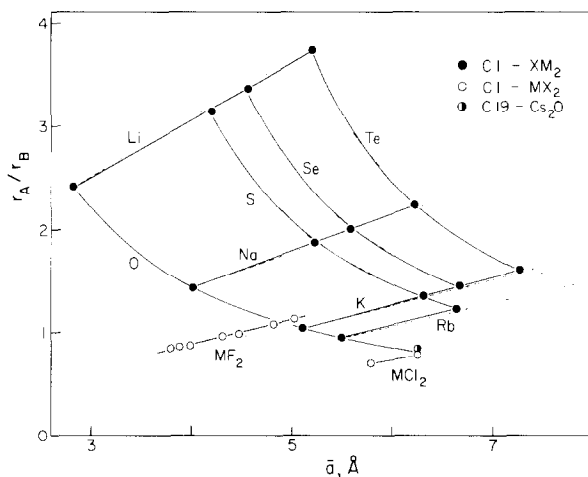


Fig. 4. Same as Fig. 3 but for the full range of r_A/r_B and \bar{a} .

structural changeover must be other than those reflected in the atomic size as represented by the empirical "effective" ionic radii.

An analogous situation exists in simple AB_2 compounds having the C 6 layer structure, not derivable by simple deformation of the fluorite structure. Here the lower R_1 (C 6) limit falls almost halfway between the ideal R_1 values for the undistorted packings: in the superconductor PdTe_2 $R = 1.270$, i.e., $R_1 = 1.555 \times \frac{1}{3} \sqrt{6}$.

To what extent the gap between the C 1 and C 19 structures can be decreased by application of external pressure does not appear to be known. The very slightly rhombohedrally distorted stoichiometric LnOF fluorites transform on heating into the disordered cubic fluorites even at pressures as high as 40 kbar (15, 16); at still higher pressures and temperatures a partial or complete conversion into a dense, probably nonstoichiometric phase of the PbCl_2 type ($Pnma$, $Z = 4$) was observed (17).

On the other hand, when A or B or both are composite ions, e.g., in $[\text{MO}_2]\text{F}_2$ ($M = \text{U, Np, Pu}$), $[\text{N}_2\text{H}_6]\text{F}_2$, or in the anti-C 19 $[\text{MeNH}_3]_2[\text{MX}_6]$ ($M = \text{Pd, Pt, Sn, Pb, Se, Te}$; $X = \text{Cl, Br, I}$) (9), the R_1 values can be much closer to $R_1(\text{C } 1) = \frac{1}{3} \sqrt{6}$ than to R_1

(C 19) $= \frac{2}{3} \sqrt{6}$. However, the tendency to form a cubic arrangement is strong. Thus the $[\text{N}_2\text{H}_6]\text{Cl}_2$ ($Pa3$) structure is a variant of the fluorite structure with ordered N_2H_7^+ ions, and similarly, $[\text{Me}_3\text{NH}]_2[\text{SnCl}_6]$ ($Pa3$, $Z = 4$; to be published) is a variant of the anti-C 1 structure with oriented Me_3NH^+ ions; the alkali and ammonium $A_2\text{MX}_6$ occur widely as $Fm3m$ antiferrofluorites, and several $(\text{Me}_4\text{N})_2\text{MCl}_6$ are also of this type. In the alkylammonium compounds the distortion of the anti-C 1 structure evidently is determined by the concerted effects of the MX_6 size and the shape of the cation rather than by a reduction in the ionic character, so that the R_1 values may be regarded—unlike in simple AB_2 compounds—as evolving in a continuous manner from R_1 (C 1), keeping in mind that a natural discontinuity will be present because of the nonexistence of substituents intermediate in size and shape between H and CH_3 .⁵ In the anti-C 1 alkylammonium compounds dipole-

⁵ Although the NO^+ ion in $(\text{NO})_2\text{MX}_6$ might be expected to give rise to rhombohedrally distorted anti-C 1 arrangements, $(\text{NO})_2\text{PtF}_6$ (18) and $(\text{NO})_2\text{PtCl}_6$ and $(\text{NO})_2\text{SnCl}_6$ (19) at room temperature have been reported as cubic and thus presumably anti-C 1, $Fm3m$ (with statically or dynamically disordered NO orientations) or $Pa3$ (ordered $(\text{NO}) \cdots X_3\text{MX}_3 \cdots (\text{NO})$

lar and hydrogen-bonding interactions result in the formation of cation $\cdots X_3MX_3 \cdots$ cation groupings with the alkyls on the outside. In the anti-C 19 crystals these groupings are aligned parallel, so that the alkyl groups form apolar layers separating the cation $\cdots X_3MX_3 \cdots$ cation sandwiches.

In MO_2F_2 ($M = U, Np, Pu$) the linear $(OMO)^+$ ions are on threefold axes. Although $M-O \sim 1.9 \text{ \AA}$, R_1 is only about 1.25. This is because the vertical extension of the OMO groups is compensated for by an interpenetration of the F and the O layers in such a way that each M atom has, in addition to the two oxygens, six nearest F neighbors at ca. 2.5 \AA forming a puckered ring about the horizontal plane passing through M . The resulting arrangement is dominated essentially by a close packing of the O and F atoms (the shortest nonmetal separations⁶ varying between ca. 2.7 and 2.8 \AA) and consists of flat FMF sandwiches separated by close-packed double layers of O atoms.

An even lower R_1 , 1.08, has been reported for $N_2H_6F_2$. The arrangement is similar to that in MO_2F_2 , but the separation of the $F \cdots H_3NNH_3 \cdots F$ sandwiches is more clear-cut. In addition, the $N_2H_6^{2+} (\bar{3}m)$ ion is hydrogen-bonded by normal $N-H \cdots F$ bonds to its six nearest F neighbors.

C 19 vs Other Structure Types

The distribution of the structure types among simple AB_2 halides, hydroxides, and alkali oxides is shown in the plots of the ionic-radius ratio r_A/r_B (Shannon's radii appropriate to the c.n.) against \bar{a} (Figs. 3 and 4). These plots are analogous to the Mooser-Pearson plots (20; cf. also Ref.

(8)) of the average principal quantum number \bar{n} against the electronegativity difference $\Delta\chi$, but the separation of the structure types is in terms of *geometric* (size) parameters.⁷ For clarity, points for the MO_2 rutiles are omitted in Fig. 3, but if included they would fall close to the points for the MF_2 rutiles. It should also be pointed out that the exact positions of the points for the C 23 ($PbCl_2$)-type structures and those for the C 6 $M(OH)_2$ hydroxides are somewhat uncertain, the former because of the irregular cation coordination and hence an ambiguous c.n., the latter because of the difficulty of assigning a realistic mean radius value to OH^- .

The separation for the compounds included in Figs. 3 and 4 is probably as clean as can be achieved in any presentation. The two figures include neither the numerous layer-type (mostly C 6) sulfides, selenides, and tellurides nor AH_2 hydrides, for the appropriate radii are difficult to assign. In this the r_A/r_B vs \bar{a} plot is less comprehensive than the corresponding Mooser-Pearson plot. On the other hand, the use of "all-purpose" electronegativity values will tend to blur the boundaries of the structure fields in the latter.

If it is assumed that, in the C 1 or anti-C 1 structures, $d(AB) = r_A + r_B$, $r_A/r_B = (K/r_B)\bar{a} - 1$ for a particular B and $[(K/r_A)\bar{a} - 1]^{-1}$ for a particular A ; $K = (3^3/4^4)^{1/6} \sim 0.687$. The pertinent lines are shown in Figs. 3 and 4, together with the best empirical fits for series with constant B (linear) and constant A (hyperbolic, $(r_A/r_B)(k_1\bar{a} - k_0) = 1$). The assumed and the empirical line for any

⁷ While the presentations are different, the results are similar. The number \bar{n} is reflected in \bar{a} : for example, for the anti-C 1 M_2X ($M = Li, Na, K$; $X = S, Se, Te$; and Rb_2S), $\bar{a} = -2.424 + 4.526\bar{n}^{1/3}$, $r^2 = 0.980$, $\sigma = 0.074 \text{ \AA}$. Furthermore, χ of the elements in a group (or period) can, in a first approximation, be represented as a linear function of the ionic radius, especially when nonempirical (electrostatic) electronegativities (21) are used. Thus if $\chi_{an} = A_0 + A_1r_{an}$ and $\chi_{cat} = C_0 + C_1r_{cat}$, $\Delta\chi = \chi_{an} - \chi_{cat} = K_0 - K_1(r_{cat}/r_{an})$ for a series with the same anion.

groupings). The unit-cell dimensions of the two hexachloro compounds are compared in Ref. (19) to those of the corresponding K salts, but the a values given cannot be correct.

⁸ It should be noted that the $z(O)$ and $z(F)$ values were chosen to give the expected interatomic distances (cf. Ref. (6)).

such series do not coincide, owing to the impossibility of deriving a universally and accurately additive set of ionic radii. The discrepancy is minimum for M_2O but significant for the M_2X chalcogenides. Analogous empirical fits were obtained for series other than C 1 and anti-C 1. It is seen that, within the limitations of the representation, these fits are quite satisfactory. Moreover, the points for a series of compounds containing a common cation can be accommodated on the same curve regardless of the structure type, e.g., CaX_2 ($X = OH, Cl, Br, I,$ and probably also F).⁸

The separation of the C 19 and C 6 compounds calls for comment. The reasons for the preference for the one or the other structure type are not well understood (for an attempted rationale cf. Ref. (22)), partly because of insufficient or unreliable experimental evidence. Leaving aside the C 6-type $M(OH)_2$ (see next section), the C 19/C 6 boundary appears to be slightly to the left of a line drawn through the points for $MnBr_2$ and $CoBr_2$. The C 19 points (excepting $TiCl_2$ and VCl_2) fall on the low- \bar{a} side of this line and the C 6 points on the high- \bar{a} side, with the exception of $NiBr_2$, NiI_2 , $ZnBr_2$, ZnI_2 , and PbI_2 (C 19). However, PbI_2 and ZnI_2 (and probably also $CoBr_2$ and $NiBr_2$) exhibit C 19/C 6 dimorphism, and there is some uncertainty about the existence of NiI_2 and $ZnBr_2$ as C 19 compounds. Practically nothing is known about the conditions of C 19/C 6 interconvertibility. There was no evidence of a transformation when CdI_2 was quenched from 500°C at pressures up to 110 kbar (2); as for the C 19/C 6 transformation of $FeCl_6$ near 2 kbar cited in Pistorius (23) comprehensive review of phase relations and structures at high pressures, reference to the original pa-

per (24) reveals that the structure of the high-pressure phase was only surmised, with no evidence of a C 6 or for that matter any other specific structure. However, it is possible that C 19/C 6 polytypism in AB_2 layer halides occurs more frequently than the available evidence would seem to indicate. A thorough reexamination of the structures and polymorphism of $TiCl_2$, VCl_2 , $NiBr_2$, NiI_2 , $ZnBr_2$, and ZnI_2 with this in mind is indicated before attempting a global explanation of the C 19 vs C 6 preference.

$M(OH)_2$: Why Not C 19?

On size criteria the $M(OH)_2$ ($M = Mg, Ca, 3d$) hydroxides would be expected to adopt structures of the C 19 type or related to rutile (Fig. 3). However, their structures are of the C 6 type. The reason for this preference may be sought in the tendency of the OH^- groups to align themselves parallel to the c axis. This alignment results in the formation of a layer of H atoms on each side of an $(HO)M(OH)$ sandwich, $\cdot \cdot \cdot |O|H| |H|O- |M|O|H| |H|O|M|O| \cdot \cdot \cdot$; these layers are analogous to the apolar layers separating the AB_2 sandwiches in the alkylammonium hexachlorostannates(IV) mentioned above. Figure 1 shows that if such an alignment were to take place in a C 19 structure the OH vectors would point with their H ends directly at the M atoms. In a C 6 structure, on the other hand, the collinearity of O, H, and M is avoided. The H atom is equidistant from three M atoms on neighboring threefold axes; the $H \cdot \cdot \cdot M$ separation is appreciably greater, and the OHM angle is significantly smaller than 180°. For example, in a C 19 structure with a, R_1 , and the positional parameters corresponding to the actual C 6 $Ca(OH)_2$ structure, the $H \cdot \cdot \cdot Ca$ distance would be ca. 2.8 Å, whereas the observed $H \cdot \cdot \cdot Ca$ distances are 3.48 Å and the OHCa angles ca. 144°.

Support for the view that the tendency to avoid OHM collinearity is a factor determining the adoption of the C 6 structure is provided by the following two observa-

⁸ The fitting of the common-cation curves for the NiX_2 to CaX_2 series was confined to compounds with the layer structures, even though the respective fluorides in fact would have been accommodated, especially if a small allowance had been made for the uncertainty in the r_A/r_{OH} ratios.

tions. The hydroxyhalides $\text{Cd}(\text{OH})\text{Cl}$ and $\text{Ca}(\text{OH})\text{Cl}$, in which the OH^- and Cl^- ions are known to be ordered and form separate OH and Cl layers, crystallize with structures of the C 27 ($\beta\text{-CdI}_2$, $P6_3mc$, $Z = 2$) type. The stacking sequence in this structure is such that a Cd and a Cl atom are found on the same threefold axis at the shortest distance of ca. 3.46 Å, while there are no Cd atoms collinear with the O–H vectors. The H atoms have three equidistant Cd (at ca. 3.75 Å, $\text{OHCd} \sim 146^\circ$) and three equidistant Cl (at ca. 2.55 Å, $\text{OHCl} \sim 124^\circ$) neighbors each. If the stacking sequence in the C 19 structure is . . . *CCCC* . . . and that in C 6 . . . *HHHH* . . . , in the C 27 structure it is . . . *HCHCHC* . . . ; the tendency of the Cd–Cl to form a C 19 and that of the Cd–OH to form a C 6 sequence are thus both satisfied. If the $\text{Cd}(\text{OH})\text{Cl}$ structure were of the C 19 type, the $\text{H} \cdots \text{Cd}$ separation in the $\text{O}—\text{H} \cdots \text{Cd}$ collinear groupings expected from the actual dimensions of $\text{Cd}(\text{OH})\text{Cl}$ would be much shorter, ca. 3.1 Å.

Second, there is circumstantial evidence

from ammonium salts. The reluctance of an N–H vector to point directly at the M atom of an MX_6 complex is well documented for the anti-C 1 (NH_4) $_2\text{MX}_6$ halides, e.g., $(\text{NH}_4)_2\text{SiF}_6$. The NH_4^+ ion has the choice of two orientations, one with the N–H vector pointing at M through an equilateral triangle of X atoms, the other with the N–H vector pointing symmetrically away from M . The latter choice is adopted in all the cases where the H atoms have been located, and there is ir spectroscopic evidence to support the structural finding (cf. Refs. (25–27)). Although one situation involves an O–H dipole carrying a net negative charge and the other an N–H group carrying a net positive charge, the orienting effect of these “dipoles” relative to M is the same in both cases.

Figure 5 illustrates the effect of the OH orientation on R_1 and \bar{a} in several hydroxyhalides. The Cd series is probably the best example:

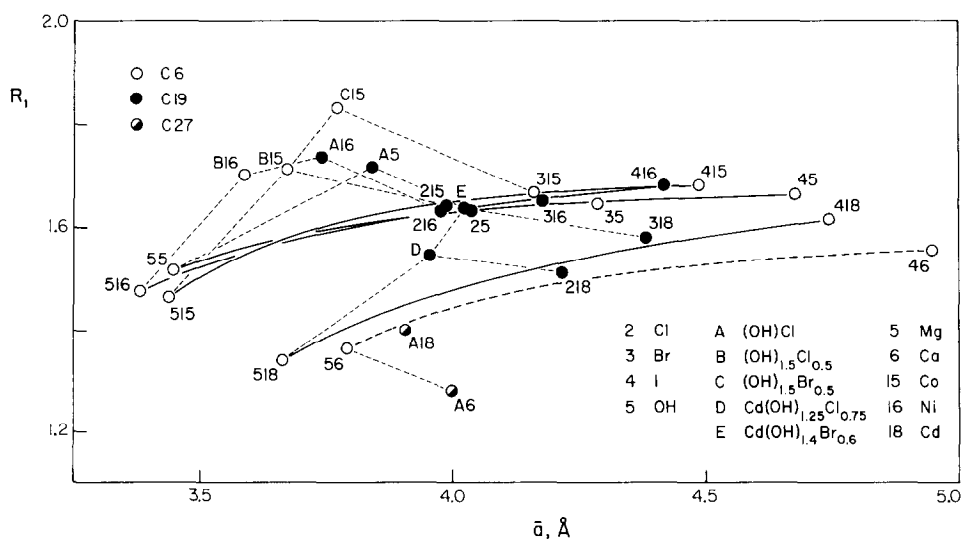
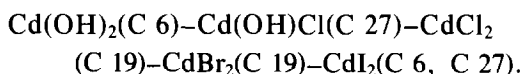


FIG. 5. Effect of OH^- on the stacking sequence in MX_2 layer structures (see text). The first digit (or letter) of the code number refers to the anion, the following digit(s) to the cation.

The structures of $\text{Cd}(\text{OH})_{1.25}\text{Cl}_{0.75}$ and $\text{Cd}(\text{OH})_{1.4}\text{Br}_{0.6}$ have been reported to be of the C 19 type; their R_1 values are unexpectedly high and \bar{a} of the chloride is larger than that of the ordered $\text{Cd}(\text{OH})\text{Cl}$ (C 27) crystal. This points to OH/ X disorder in the C 19 structure. Similarly, R_1 of $\text{Ca}(\text{OH})\text{Cl}$ (ordered, C 27) is even lower than R_1 of $\text{Ca}(\text{OH})_2$ if the reported unit-cell dimensions can be relied upon. In contrast, the R_1 values of the Mg, Co, and Ni hydroxyhalides included in Fig. 5 are all substantially higher than would be expected from their respective \bar{a} values, indicating the existence of disorder even at OH: X ratios of unity. It is not clear whether or not there is any tendency toward anion ordering within the mixed OH, X layers. The changeover from C 6 in $M(\text{OH})_2$ to C 19 in $M(\text{OH})X$ for phases of intermediate compositions undoubtedly is influenced by the relative sizes of M and X and probably involves a fine balance of these and other factors.

A_2MX_6 : Why Not Anti-C 19?

The anti-C 19-type structure does not appear to be adopted by any of the many A_2MX_6 compounds, even though some of them exist in as many as three polymorphs.⁹ However, the anti-C 6 structure is well represented among A_2MF_6 and A_2MCl_6 . Because of the size of the MX_6 anion the a dimension in these compounds is large, but the c dimension does not increase in proportion: the vertical separation of adjacent A and X layers in an $A \cdots X-M-X \cdots A$ sandwich is only 0.2–0.6 Å in the fluorides and almost zero in the chlorides. This results in R_1 values which are quite low, 0.78–0.83 (i.e., close to $\frac{1}{3}\sqrt{6}$),

⁹ For example, K_2MnF_6 , Cs_2VF_6 , and Rb_2TiF_6 each occur as anti-C 6, anti-C 27, and anti-C 1 polymorphs. The Madelung constants and the densities of the polymorphs decrease in this order, which also appears to be the order of the thermal stability ranges of these structures (cf. Ref. (10)).

compared to those of simple AB_2 (C 6) compounds (Fig. 2).

Attempts to explain the conspicuous absence of the C 19 structure in A_2MX_6 on steric grounds are at present hampered by the uncertainties of the available information on the metric aspects of the C 6 structures, but the following observation may be relevant. In a C 6 structure the cation atom A is on a threefold axis and coordinated by $3 + 6 + 3 X$ atoms. The six X atoms ($z(X_1) \sim \frac{1}{4}$) are contributed in pairs by three MX_6 anions and are almost coplanar with A ($z(A) \sim \frac{1}{4}$). One set of three X ($z(X_2) = -z(X_1)$) belongs to the same three MX_6 groups and forms an equilateral $X_2X_2X_2$ triangle below the $A \cdots 6X_1$ quasi-plane. The other set of three X ($z(X_3) = 1 - z(X_1)$) is contributed by three other MX_6 groups and forms an equilateral $X_3X_3X_3$ triangle above the $A \cdots 6X_1$ quasi-plane. In this $A \cdots 12X$ configuration the A atom "sees" three M atoms through the planes of three equivalent $X_1X_1X_2$ triangles at a distance $M \cdots A = [\frac{2}{3}a^2 + z_A^2c^2]^{1/2}$ and at AMA angles not far from tetrahedral, and a fourth M through the plane of the $X_3X_3X_3$ triangle, at a much larger distance $M' \cdots A = [\frac{8}{3}a^2 + c^2(1 - z_A)^2]^{1/2}$. The $A \cdots X_1$, $A \cdots X_2$, and $A \cdots X_3$ distances in a particular crystal are quite similar in the chlorides; in the fluorides the difference between the shortest and the longest $A \cdots F$ distance appears to be of the order of 3–6% in any one compound.¹⁰

If a , R_1 , $x(X)$, $z(X)$, and $z(A)$ remained the same as in the C 6 structure but adjacent $A \cdots X-M-X \cdots A$ layers were displaced so as to form a C 19 sequence, the $A \cdots X_1$ distances would remain unchanged but the $A \cdots X_3$ distances in the fluorides would become shorter by up to ca. 17% and the $A \cdots X_2$ distances by up to

¹⁰ The $(\text{NH}_4)_2MX_6$ present the additional complication of trifurcated $\text{N}-\text{H} \cdots 3X$ bonding (cf. Refs. (26) and (27)). The difference in the $A \cdots X$ distances in the fluorides is larger, in excess of 6%.

TABLE I
 AB_2 STRUCTURE TYPES REPRESENTED AMONG
 ALKYLAMMONIUM HEXAHALOMETALLATES(IV)^{a,b}

$R\bar{3}m \subset Fm\bar{3}m$ anti-C 1		$C 2 \rightarrow C 1$ if $x(B) = \frac{1}{4}$ ^c
$Fm\bar{3}m, Z = 4$ $(NH_4)_2SnCl_6$ (28) $(Me_4N)_2SnCl_6$ (29, 30) $(Me_4N)_2SiF_6, I4/m = F4/m \subset Fm\bar{3}m$ (31) $(Me_4N)_2TeBr_6, Fd\bar{3}c$ (30) $(Me_4N)_2ReBr_6, I4_1/acd \subset Fd\bar{3}c$ (32) $(Et_4N)_2SnCl_6, C2/c$ (32) $*(Et_3NH)_2SnCl_6, P2_1/n$ (12)		
$R\bar{3}m \subset Pa\bar{3}$		
anti-C 19		anti-C 2
$R\bar{3}m, Z = 1$ $*(MeNH_3)_2MX_6$ (9)		$Pa\bar{3}, Z = 4$ $*(Me_3NH)_2SnCl_6$ (33)
anti-C 6		anti-C 18 or anti-C 35
$P\bar{3}m1, Z = 1$ $\beta-(NH_4)_2SiF_6$ $*(EtNH_3)_2SnCl_6$ (34) $*(n-PrNH_3)_2SnCl_6, P2_1$		$Pnmm, Z = 2$ $*(Me_2NH_2)_2SnCl_6$ (35)
other		
$*(n-Pr_3NH)_2SnCl_6, C2/c$		

^a C 1, CaF_2 ; C 2, FeS_2 (pyrite); C 6, CdI_2 ; C 18, FeS_2 (marcasite); C 19, $CdCl_2$; C 35, $CaCl_2$.

^b The asterisks refer to our own recent crystal-structure determinations (Ref. (12) and to be published).

^c For simple AB_2 compounds.

ca. 13%, i.e., below—in some cases well below—the sum of the ionic radii. In the chlorides, where the packing is probably dominated by $Cl \cdots Cl$ contacts, both $A \cdots X_2$ and $A \cdots X_3$ would increase somewhat, up to ca. 5%, with the result that all three $A \cdots Cl$ distances would be more closely similar. At the same time, however, the A atom in both the fluorides and chlorides would “see” the fourth M atom through the triangle of $X_3X_3X_3$ atoms, this time all three belonging to the same MX_6 , at an $M' \cdots A$ distance $(1 - z_A)c$ which is not only shorter than the $M' \cdots$

A distance in the C 6 structure, but drastically shorter than even the $M \cdots A$ distance in C 6. For example, in K_2PtF_6 (C 6), $Pt \cdots K \sim 4.5 \text{ \AA}$, $Pt' \cdots K \sim 5.5 \text{ \AA}$; in K_2PtF_6 (C 19), $Pt \cdots K$ would remain unchanged, while $Pt' \cdots K$ would decrease to ca. 3.4 \AA . Similarly, in Cs_2ThCl_6 , $Th \cdots Cs \sim 5.9 \text{ \AA}$ and $Th' \cdots Cs \sim 7.3 \text{ \AA}$, but in the hypothetical C 19 variant $Th' \cdots Cl$ would be ca. 4.5 \AA . Clearly the structural parameters would not remain the same on the C 6 \rightarrow C 19 conversion, but the changes would be expected to be small because of the constraints imposed by the

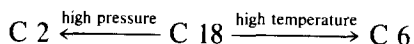
essentially constant $M-X$ distances, $X \cdots X$ contacts, and MXM angles. Considering that the $M' \cdots A$ distances calculated on the above assumptions are almost 40% shorter than the observed distances, it seems probable that even with adjustments in a , R_1 , and the positional parameters the C 19 configuration would be unfavorable compared with the C 6 configuration. This may well be the reason for the absence of A_2MX_6 (C 19) from the reported A_2MX_6 structures.¹¹

$(R_nNH_{4-n})_2MX_6$: A Structural AB_2
Minicosmos

While in the $(MeNH_3)_2MX_6$ compounds there is a tendency to modify the parent anti-C 1-type structure to anti-C 19, replacement of Me by a longer-chain alkyl may take the structure alteration a step further, e.g., to the anti-C 6 type, as in $(EtNH_3)_2SnCl_6$ and $(n-PrNH_3)_2SnCl_6$. The simpler alkylammonium hexahalometalates(IV) in fact represent a surprising range of the structural alternatives (including distorted varieties) encountered in simple AB_2 compounds, if one disregards the composite nature of the cation and anion and considers the structures as consisting of arrangements of charge centroids. This is illustrated in Table I. $(RNH_3)_2MX_6$ containing R with chains longer than n -propyl have not yet been studied, but their room-temperature structures may well turn out to be variants of the C 6 structure with the alkyl chains of effective cylindrical symmetry arranged in parallel close-packed hexagonal arrays.

Although the C 6 and C 18 types represented in Table I are not derivable by dis-

tortion from C 1, the kinship of these structures in simple AB_2 compounds is demonstrated by the existence of polymorphic transformations such as those in $CoTe_2$:



(cf. also Ref. (36)). Information on corresponding transformations in the alkylammonium compounds so far is lacking, though $(MeNH_3)_2TeCl_6$ (C 6) has been reported to transform on cooling to 105K into a C 19 structure containing stacking faults; on heating the crystal did not revert to the C 6 form until 230K (37).

A fuller discussion of the crystal chemistry and ir spectroscopy of the $(R_nNH_{4-n})_2MX_6$ halides will appear elsewhere in the near future.

References

1. V. M. GOLDSCHMIDT, "Handwörterbuch der Naturwissenschaften," 3rd ed., Vol. 5, pp. 1128-1154, Fischer, Jena, 1934. [Cited in Ref. (2)].
2. K.-F. SEIFERT, *Fortschr. Mineral.* **45**, 214 (1968).
3. L. PAULING, "The Nature of the Chemical Bond," 3rd ed., Cornell Univ. Press, Ithaca, N.Y., 1960.
4. R. C. EVANS, "An Introduction to Crystal Chemistry," 2nd ed., Cambridge Univ. Press, Cambridge, 1966.
5. P. NIGGLI, "Lehrbuch der Mineralogie und Kristallographie," 3rd ed., Vol. 1, Borntraeger, Berlin, 1941.
6. R. W. G. WYCKOFF, "Crystal Structures," 2nd ed., Vols. 1-5, Interscience, New York, 1963-1966.
7. A. F. WELLS, "Structural Inorganic Chemistry," 4th ed., Oxford Univ. Press, Clarendon, London/New York, 1975.
8. D. M. ADAMS, "Inorganic Solids," Wiley, London/New York, 1974.
9. Y. KUME, R. IKEDA, AND D. NAKAMURA, *J. Magn. Reson.* **33**, 331 (1979).
10. D. BABEL, *Struct. Bonding* **3**, 1 (1967).
11. W. B. PEARSON, "The Crystal Chemistry and Physics of Metals and Alloys," Wiley-Interscience, New York/London, 1972.
12. O. KNOP, T. S. CAMERON, M. A. JAMES, AND M. FALK, *Canad. J. Chem.* **59**, 2550 (1981).

¹¹ A similar argument would of course apply to the anti-C 27 structure, but to a lesser extent: the structure is polar and a possibility of asymmetric adjustment of the vertical $M \cdots A$ distances exists. Accurate determinations would be required to test the reasonability of the argument in this case.

13. W. B. PEARSON, "A Handbook of Lattice Spacings and Structures of Metals and Alloys," Vols. 1-2, Pergamon, New York/London, 1958-1967.
14. R. D. SHANNON, *Acta Crystallogr. Sect. A* **32**, 751 (1976).
15. D. B. SHINN AND H. A. EICK, *Inorg. Chem.* **8**, 232 (1969).
16. C. W. F. T. PISTORIUS, *J. Less-Common Met.* **31**, 119 (1973).
17. M. GONDRAND, J. C. JOUBERT, J. CHENAVAS, J. J. CAPPONI, AND M. PERROUD, *Mater. Res. Bull.* **5**, 769 (1970).
18. F. P. GORTSEMA AND R. H. TOENISKOETTER, *Inorg. Chem.* **5**, 1217 (1966).
19. D. W. A. SHARP AND J. THORLEY, *J. Chem. Soc.* 3557 (1963).
20. E. MOOSER AND W. B. PEARSON, *Acta Crystallogr.* **12**, 1015 (1959).
21. R. J. BOYD AND G. E. MARKUS, *J. Chem. Phys.* **75**, 5385 (1981).
22. H. KREBS, "Grundzüge der anorganischen Kristallchemie," F. Enke Verlag, Stuttgart, 1968. [Engl. transl.: "Fundamentals of Inorganic Crystal Chemistry," McGraw-Hill, New York, 1968].
23. C. W. F. T. PISTORIUS, *Prog. Solid State Chem.* **11**, 1 (1976).
24. A. NARATH AND J. E. SCHIRBER, *J. Appl. Phys.* **37**, 1124 (1966).
25. O. KNOP, W. J. WESTERHAUS, AND M. FALK, *Canad. J. Chem.* **58**, 270 (1980).
26. O. KNOP, W. J. WESTERHAUS, AND M. FALK, *Canad. J. Chem.* **58**, 867 (1980).
27. O. KNOP, I. A. OXTON, W. J. WESTERHAUS, AND M. FALK, *J. Chem. Soc. Faraday* **2** **77**, 811 (1981).
28. J. A. LERBSCHER AND J. TROTTER, *Acta Crystallogr. Sect. B* **32**, 2671 (1976).
29. T. R. BRILL, R. C. GEARHART, AND W. A. WELSH, *J. Magn. Reson.* **13**, 27 (1974).
30. R. W. BERG AND K. NIELSEN, *Acta Chem. Scand. A* **33**, 157 (1979).
31. R. B. COREY, *Z. Kristallogr.* **89**, 10 (1934).
32. H. SOWA, U. DRÜCK, AND A. KUTOGLU, *Cryst. Struct. Comm.* **10**, 699 (1981).
33. R. W. G. WYCKOFF AND R. B. COREY, *Amer. J. Sci.* **18**, 437 (1929).
34. R. W. G. WYCKOFF, *Z. Kristallogr.* **68**, 231 (1928).
35. M. H. BEN GHOZLEN, A. DAOUD, AND J. W. BATS, *Acta Crystallogr. Sect. B* **37**, 1415 (1981).
36. A. KJEKSHUS AND T. RAKKE, *Struct. Bonding* **19**, 85 (1974).
37. K. KITAHAMA AND H. KIRIYAMA, *Acta Crystallogr. Sect. A* **34**, S302 (1978).